

Exploring H₂-effects on radiation-induced oxidative dissolution of UO₂-based spent nuclear fuel using numerical simulations

N.L. Hansson^a, M. Jonsson^{b,*}

^a Nuclear Chemistry / Industrial Materials Recycling, Chalmers University of Technology, SE-412 96, Gothenburg, Sweden

^b School of Engineering Sciences in Chemistry, Biotechnology and Health, Department of Chemistry, KTH Royal Institute of Technology, SE-100 44, Stockholm, Sweden

ARTICLE INFO

Handling Editor: Dr. Jay Laverne

Keywords:

Oxidative dissolution

UO₂

H₂O₂

Hydrogen effect

Surface bound hydroxyl radical

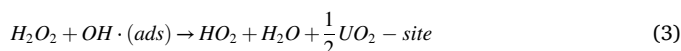
ABSTRACT

Using a recently developed approach for numerical simulation of radiation-induced oxidative dissolution of spent nuclear fuel, we have explored the impact of three possible contributions to the inhibiting effect of molecular hydrogen. The three contributions are (1) effect on oxidant production in irradiated water, (2) reduction of oxidized uranium catalyzed by noble metal inclusions (fission products) and (3) reaction with surface-bound hydroxyl radicals preventing the oxidation of uranium. The simulations show that the first contribution is of fairly small importance while the second contribution can result in complete inhibition of the oxidative dissolution. This is well in line with previous work. Interestingly, the simulations imply that the third contribution, the reaction between H₂ and the surface-bound hydroxyl radical formed upon reaction between the radiolysis product H₂O₂ and UO₂, can account for the inhibition observed in systems where noble metal inclusions are not present. This is discussed in view of previously published experimental data.

1. Introduction

Handling the long-term radiotoxic used nuclear fuel is one of the main challenges of the nuclear industry. Several countries have decided to use a once-through nuclear fuel cycle where the used nuclear fuel is placed in a geological repository until the radiotoxicity level has decreased to levels corresponding to a natural uranium ore. This means that the repository must stay intact for 10⁵–10⁶ years. To achieve this, a combination of natural and engineered barriers is used. The licensing process relies on safety assessments accounting for various scenarios. One unlikely, yet very relevant, scenario is complete barrier failure allowing groundwater intrusion into the canister containing the used nuclear fuel. Most fuels are based on UO₂. After use in a reactor, only a few percent of the material has been transformed into fission products and heavier actinides. Therefore, the chemical behavior of used nuclear fuel exposed to groundwater can be expected to be similar to that of UO₂. In the slightly reducing groundwaters found at several potential repository sites, the solubility of UO₂ is very low and one would expect very slow dissolution of the fuel matrix. However, the highly radioactive fission products and heavier actinides present induce radiolysis of the surrounding groundwater, producing oxidants (OH•, HO₂• and H₂O₂) and reductants (e_{aq}⁻, H• and H₂). For kinetic reasons, the oxidants will

dominate the initial surface chemistry and oxidize the sparsely soluble UO₂ to significantly more soluble U(VI) and thereby induce oxidative dissolution of the fuel matrix. This process has been extensively studied for decades and the level of mechanistic understanding can be considered to be fairly high. According to some of the more recent studies, the radiolytic oxidant driving the process is primarily H₂O₂ and the mechanism involves the formation of surface-bound hydroxyl radicals as a common intermediate for oxidation of UO₂ and catalytic decomposition of H₂O₂ (Ekeröth et al., 2006; Barreiro Fidalgo et al., 2018). These reactions are summarized below.



The adsorption site for H₂O₂ is referred to as UO₂ – site and the surface-bound hydroxyl radical is referred to as OH•(ads). In systems where significant amounts of UO₂²⁺ are present in solution, H₂O₂ can form ternary complexes with UO₂²⁺ and HCO₃⁻/CO₃²⁻ or with UO₂²⁺ and

* Corresponding author.

E-mail address: matsj@kth.se (M. Jonsson).

<https://doi.org/10.1016/j.radphyschem.2023.111055>

Received 11 April 2023; Received in revised form 17 May 2023; Accepted 22 May 2023

Available online 23 May 2023

0969-806X/© 2023 The Authors. Published by Elsevier Ltd. This is an open access article under the CC BY license (<http://creativecommons.org/licenses/by/4.0/>).

Cl^- in salt brines (Zanonato et al., 2012). It has been shown that the reactivity of H_2O_2 towards the UO_2 -surface is attributed to the fraction of free H_2O_2 (Olsson et al., 2022). Complexed H_2O_2 appears to be significantly less reactive.

In general, the overall mechanism for the radiation chemistry of water and the surface reactions involved in oxidative dissolution of the fuel matrix is quite complex. Therefore, numerical models are required for the safety assessment. Very recently, we developed a numerical model with spatial and temporal resolution taking the geometrical dose distribution, radiation chemistry of water and surface reactions into account (Hansson et al., 2023). The surface reactions are described on the basis of the mechanism above. This model can be regarded as a starting point for exploring the potential impact of groundwater constituents.

Molecular hydrogen is a radiolysis product, and it can also be formed upon anoxic corrosion of iron-containing materials. Since canisters for used nuclear fuel are usually constructed with a cast-iron insert for mechanical support, complete barrier failure implies contact between anoxic groundwater and iron. As the depth of the geological repositories is usually hundreds of meters, considerable concentrations of H_2 can be produced before gas bubbles are formed (Bonin et al., 2000). Hence, H_2 can become a major groundwater constituent inside a breached canister. There are numerous experimental studies showing that H_2 can retard or completely inhibit radiation-induced oxidative dissolution of UO_2 -based materials (Cui et al., 2008; Röllin et al., 2001; Carbol et al., 2005; Broczkowski et al., 2005; Trummer et al., 2008; Eriksen et al., 2008; Muzeau et al., 2009; Carbol et al., 2009b). The impact of H_2 on the process has partly been attributed to the radiolysis of water where H_2 will affect the production of oxidants. It has also been shown that fission products present as noble metal inclusions can catalyze the reduction of oxidized UO_2 by H_2 . The noble metal inclusions are referred to as ϵ -particles and consist of Mo, Tc, Rh, Ru and Pd solid solution. This should be the main effect and complete inhibition is expected already at very low H_2 concentrations. The noble metal inclusions have also been proposed to catalyze the reaction between H_2O_2 and H_2 as well as the oxidation of UO_2 by both H_2O_2 and O_2 (Trummer et al., 2008, 2009; Nilsson and Jonsson, 2008a, 2008b; Maier and Jonsson, 2019). A third mechanism that has been discussed is the reaction between H_2 and the surface-bound hydroxyl radical (Bauhn et al., 2018a). This reaction would compete with the oxidation of U(IV) as well as the reaction between H_2O_2 and the surface-bound hydroxyl radical and thereby slow-down the oxidative dissolution.

In this work we have added the two surface processes that are believed to contribute to the observed H_2 effect to the recently developed model. Simulations are performed in order to assess the relative importance of the three H_2 effects mentioned above.

2. Method and models

UO_2 fuel with a dose rate of 1 Gy/h, 5.5 MeV α -particle energy as well as 95% theoretical density was modelled. The numerical model and the parameters on which it is based are described in detail in Hansson et al. (2023). A UO_2 surface site density of $2.1 \cdot 10^{-4} \text{ mol m}^{-2}$ derived in the work of Hossain et al. was used (Hossain et al., 2006). All surface concentrations were expressed using the $\text{S} \cdot \text{V}^{-1}$ ratio in combination with the surface site density. In all simulations a 50 μm single layer system was modelled for 10^3 steps of 100 s each.

The reactions in the $\text{H}_2\text{O}_2/\text{UO}_2$ system are reactions (1)–(3). The rate constants for these reactions are referred to as ks1 , ks2 and ks3 . Reaction (4) is a homogeneous reaction in solution. This reaction and the corresponding rate constant are already included in the general radiolysis model (Hansson et al., 2023). As the product of reaction (2) is U(V) , we must also include a surface disproportionation reaction to produce soluble U(VI) (Li et al., 2023). This reaction is written as $\text{U(V)}\text{O}_2 + \text{U(V)}\text{O}_2 \rightarrow \text{U(VI)}\text{O}_2(\text{s})$ with a rate constant denoted ks4 .

Based on fitting to experimental data, the rate constants were

previously determined to $\text{ks1} = 0.462 \text{ M}^{-1} \text{ s}^{-1}$, $\text{ks2} = 0.191 \text{ s}^{-1}$, $\text{ks3} = 197 \text{ M}^{-1} \text{ s}^{-1}$ and $\text{ks4} = 34.1 \text{ M}^{-1} \text{ s}^{-1}$ (Hansson et al., 2023). To quantify the reactive surface the solid surface area to solution volume ratio and a previously determined reactive site density have been used.

The reactions that are required to simulate the impact of H_2 on radiation induced dissolution of UO_2 are presented below. In the original version of the model, the rate of dissolution of oxidized uranium was not an issue as there were no competing reactions. Therefore, U(VI) was assumed to dissolve as soon as it was formed (Hansson et al., 2023). However, to describe the noble metal particle catalyzed reduction of U(VI) back to U(IV) we must also consider the kinetics for U(VI) dissolution since this is a competing reaction. In a system containing HCO_3^- , the rate of U(VI) dissolution will depend on the HCO_3^- concentration (Hossain et al., 2006) and the rate limiting step can be described as a bimolecular reaction between HCO_3^- and oxidized UO_2 . The reaction between H_2 and the surface-bound hydroxyl radical can simply be described in the same way as the corresponding reaction for H_2O_2 (i.e., analogous to reaction (3)). The noble metal particle catalyzed reduction of U(VI) by H_2 and oxidation of U(IV) by H_2O_2 are a bit more complicated to describe. Experimentally, the rate limiting step has been found to be the encounter between the solute (H_2 or H_2O_2) the noble metal particle (Trummer et al., 2008). To account for this experimental observation, both processes have been divided into two reactions each where the first reaction is rate determining. In the reactions involving noble metal particles, ϵ – site denotes the noble metal particle. In the reaction with H_2 , a hypothetical product “red” is formed while in the reaction with H_2O_2 , a hypothetical product “ox” is formed. The reducing product “red” rapidly reduces U(VI) to U(IV) while the oxidizing product “ox” rapidly oxidizes U(IV) to U(VI) . This is a way of enabling a system with only bimolecular (or unimolecular) reactions as well as a way of maintaining a realistic mass balance. The reactions mentioned above are summarized in Table 1.

The rate constants of these reactions are discussed in the next section.

3. Results and discussion

3.1. Rate constants

The dissolution of UO_2^{2+} in carbonate solution, described as a bimolecular reaction between HCO_3^- and U(VI) on the surface as written in Table 1, has been found to be close to diffusion controlled (Hossain et al., 2006). Therefore, we set the value for $\text{ks5} = 10^3 \text{ M}^{-1} \text{ s}^{-1}$ which corresponds to the diffusion controlled rate constant for a reaction between a solute and the surface in this particular heterogeneous system (i.e., the system for which ks1 – ks4 were determined) (Jonsson, 2010). The rate constant for the reaction between H_2 and the surface-bound hydroxyl radical, ks6 , is not known experimentally. However, from homogeneous reactions in solution we know that the rate constant for the reaction between the hydroxyl radical and H_2 is more or less the same as the rate constant for the reaction between the hydroxyl radical and H_2O_2 (Christensen et al., 1982; Christensen and Sehested, 1983). Based on this, ks6 could be set equal to ks3 . However, the surface-bound hydroxyl radical has been shown to be considerably less reactive than the free hydroxyl radical. The reduction potential of the surface-bound hydroxyl radical is more than 300 mV lower than for the free hydroxyl radical

Table 1

The extended surface site reaction system with epsilon particle reactions.

$\text{HCO}_3^- + \text{U(VI)}\text{O}_2(\text{s}) \rightarrow \text{UO}_2\text{CO}_3(\text{aq}) + \text{UO}_2 - \text{site}$	ks5
$\text{OH} \cdot (\text{ads}) + \text{H}_2 \rightarrow \text{H} \cdot + \frac{1}{2} \text{UO}_2 - \text{site} + \text{H}_2\text{O}$	ks6
$\epsilon - \text{site} + \text{H}_2 \rightarrow \text{red}$	ks7
$\text{red} + \text{U(VI)}\text{O}_2(\text{s}) \rightarrow \text{UO}_2 - \text{site} + 2\text{H}^+ + \epsilon - \text{site}$	ks8
$\text{H}_2\text{O}_2 + \epsilon - \text{site} \rightarrow \text{ox}$	ks9
$\text{ox} + \text{UO}_2 - \text{site} \rightarrow \text{U(VI)}\text{O}_2(\text{s}) + \epsilon - \text{site} + 2\text{OH}^-$	ks10

(Lawless et al., 1991). This would imply that hydrogen abstraction from H_2 would not be an exothermic reaction for the surface-bound hydroxyl radical while hydrogen abstraction from H_2O_2 still would be. Hence, it is likely that ks_6 is considerably lower than ks_3 . To account for all possibilities, ks_6 has been varied between 0 and $10^3 \text{ M}^{-1} \text{ s}^{-1}$.

Experimental work on UO_2 pellets containing Pd-particles to mimic the effects of noble metal inclusions have shown that the reaction between H_2 and the noble metal inclusions is close to diffusion controlled (Trummer et al., 2008). In other words, ks_7 should be close to $10^3 \text{ M}^{-1} \text{ s}^{-1}$ (the limit for a diffusion controlled rate constant in this system). The subsequent reaction ($red + U(VI)O_2(s)$) should have a rate constant high enough not to affect the reduction of $U(VI)$ (i.e., not to become rate-determining) but low enough not to cause numerical problems. A value of $ks_8 = 10^{16} \text{ M}^{-1} \text{ s}^{-1}$ was found to satisfy these boundary conditions.

Work on the same Pd-containing UO_2 pellets also showed that the noble metal catalyzed oxidation of $U(IV)$ by H_2O_2 has a rate constant 100 times higher than that of the direct reaction between H_2O_2 and UO_2 (Trummer et al., 2008). For this reason, ks_9 is set to 100 times that of ks_1 . The subsequent reaction ($ox + U(IV)O_2(s)$) has the same rate constant as ks_8 since it must satisfy the same boundary conditions.

3.1.1. Impact of H_2 on the radiolytic production of oxidants

The impact of H_2 on the oxidative dissolution of UO_2 was explored using the original version of the model (i.e., without the reactions presented in Table 1). In this version, oxidized UO_2 is assumed to dissolve instantly. This is a reasonable assumption for systems containing 10 mM HCO_3^- but not for systems with HCO_3^- concentrations lower than 1 mM (Hossain et al., 2006). In Table 2, the absolute dissolution rates for the system without initial H_2 at different dose rates are given along with the relative dissolution rates at different initial H_2 pressures.

As can be seen, H_2 appears to increase the rate of dissolution slightly for dose rates up to $2.78 \cdot 10^{-2} \text{ Gy s}^{-1}$. This effect is only present in solutions with HCO_3^- , which can scavenge the radicals that cause a protective effect towards H_2O_2 under relatively low dose rates. At higher dose rates and at H_2 pressures above 1 bar, the relative dissolution rate is reduced.

Impact of H_2 reacting with surface-bound hydroxyl radicals.

As stated above, it is reasonable to assume that the rate constant for the reaction between H_2 and the surface-bound hydroxyl radical, ks_6 , should be lower than the corresponding rate constant for H_2O_2 , ks_3 . In any case, the rate constant cannot exceed what is defined as diffusion controlled in the current system. To explore the impact of this reaction on the dissolution of UO_2 , simulations were performed at a range of ks_6 from 0 to $10^3 \text{ M}^{-1} \text{ s}^{-1}$ at 40 bar H_2 . The results are shown in Fig. 1.

As can be seen, the maximum possible impact of this reaction is a reduction of the dissolution rate by slightly more than two orders of magnitude. However, it is more reasonable to use a rate constant lower than ks_3 . In the following, we have used a rate constant of $50 \text{ M}^{-1} \text{ s}^{-1}$ which is 25% of ks_3 . To further explore the impact of this reaction we have determined the steady-state dissolution rate of uranium at different H_2 pressures using $ks_6 = 50 \text{ M}^{-1} \text{ s}^{-1}$. The results are summarized in Table 3.

It is interesting to note that the dissolution rate at 0 bar initial H_2 is also affected by including the reaction between H_2 and the surface-

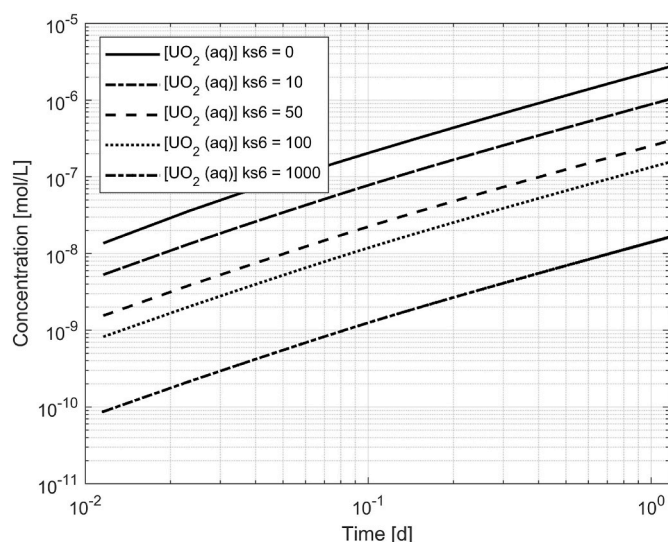


Fig. 1. Different constants for ks_6 , and its influence on the dissolution of UO_2 considering no ϵ -particles and a value for $ks_5 = 10^3 \text{ M}^{-1} \text{ s}^{-1}$ in a 50 μm single layer system with 100 s time steps.

bound hydroxyl radical at higher dose rates. This can be attributed to radiolytically produced H_2 .

Looking at the impact of different initial H_2 pressures it is evident that the relative dissolution rate decreases with increasing H_2 pressure for all dose rates included in the study. It is also evident that the reduction in dissolution rate is most significant at the highest dose rate. However, it should be noted that the main part of this reduction is seen already at 0 bar initial H_2 . At dose rates up to $2.78 \cdot 10^{-2} \text{ Gy s}^{-1}$, 40 bar H_2 reduces the rate of dissolution by one order of magnitude. At higher dose rates, the reduction approaches two orders of magnitude.

Impact of noble metal particle catalyzed reactions.

The noble metal particle catalyzed reduction of $U(VI)$ by H_2 on the surface of UO_2 has previously been claimed to be the major H_2 effect (Trummer and Jonsson, 2010). As discussed above, the fission products present as noble metal inclusions also catalyze oxidation of UO_2 . To explore the impact of noble metal particle catalyzed reactions we simulated the system taking also these reactions into account. The results at 0 bar initial H_2 are summarized in Table 4.

From this table it is evident that the noble metal particle catalyzed reduction of $U(VI)$ is quite effective already when water radiolysis is the only source of H_2 . At the highest ks_7 (diffusion controlled), oxidative dissolution is effectively inhibited at all dose rates studied while for $ks_7 = 10^2 \text{ M}^{-1} \text{ s}^{-1}$, oxidative dissolution still occurs at the three highest dose rates. However, the rate of dissolution is reduced 1-2 orders of magnitude. Simulations at the initial H_2 pressures shown in Table 3 show that the oxidative dissolution is completely inhibited in all cases. To illustrate the efficiency of the inhibition we have identified the minimum initial H_2 pressure required to suppress oxidative dissolution of UO_2 at different dose rates and noble metal particle surface coverage. The results are shown in Table 5.

Table 2

Dissolution rates and relative dissolution rates under varying dose rates and H_2 pressures in 10 mM $NaHCO_3$ solution without H_2 surface reactions.

D [Gy s^{-1}]	Relative dissolution rate 10 mM $NaHCO_3^-$					
	Dissolution rate [$\text{mol m}^{-2} \text{s}^{-1}$]	1 [bar]	5 [bar]	10 [bar]	20 [bar]	40 [bar]
$2.78 \cdot 10^{-5}$	$1.2 \cdot 10^{-13}$	1.00	1.01	1.03	1.04	1.05
$2.78 \cdot 10^{-4}$	$1.2 \cdot 10^{-12}$	1.04	1.10	1.11	1.12	1.12
$2.78 \cdot 10^{-3}$	$1.2 \cdot 10^{-11}$	1.06	1.10	1.10	1.10	1.10
$2.78 \cdot 10^{-2}$	$1.3 \cdot 10^{-10}$	1.06	1.07	1.06	1.05	1.04
$2.78 \cdot 10^{-1}$	$1.3 \cdot 10^{-9}$	1.02	0.93	0.87	0.80	0.75
2.78	$1.2 \cdot 10^{-8}$	1.00	0.80	0.61	0.41	0.27

Table 3Relative dissolution rates (compared to 0 bar H₂ and ks6 = 0) in 10 mM NaHCO₃ using ks6 = 50 M⁻¹ s⁻¹.

D [Gy·s ⁻¹]	Dissolution rate [mol·m ⁻² ·s ⁻¹] ^a	Relative dissolution rate				
		1 [bar]	5 [bar]	10 [bar]	20 [bar]	40 [bar]
2.78·10 ⁻⁵	1.2·10 ⁻¹³	0.84	0.51	0.35	0.21	0.12
2.78·10 ⁻⁴	1.2·10 ⁻¹²	0.90	0.55	0.37	0.22	0.12
2.78·10 ⁻³	1.2·10 ⁻¹¹	0.91	0.54	0.35	0.21	0.12
2.78·10 ⁻²	1.3·10 ⁻¹⁰	0.86	0.48	0.31	0.18	0.09
2.78·10 ⁻¹	8.7·10 ⁻¹⁰	0.56	0.29	0.18	0.10	0.05
2.78	1.2·10 ⁻⁹	0.10	0.08	0.06	0.03	0.02

^a Dissolution rates at 0 bar initial H₂ and ks6 = 50 M⁻¹ s⁻¹.**Table 4**

Dissolution rates as a function of dose rate with varying constants ks6 and ks7 with 1% ε-particle surface coverage.

Dose rate (Gy·s ⁻¹)	Dissolution rate [mol·m ⁻² ·s ⁻¹]				
	ks6 = 0, ks7 = 0	ks6 = 50, ks7 = 0	ks6 = 50, ks7 = 10 ²	ks6 = 50, ks7 = 10 ³	ks6 = 50, ks7 = 10 ⁴
2.78·10 ⁻⁵	1.2·10 ⁻¹³	1.2·10 ⁻¹³	2.5·10 ⁻²²	1.2·10 ⁻²²	1.2·10 ⁻²²
2.78·10 ⁻⁴	1.2·10 ⁻¹²	1.2·10 ⁻¹²	2.6·10 ⁻²²	1.2·10 ⁻²²	1.2·10 ⁻²²
2.78·10 ⁻³	1.2·10 ⁻¹¹	1.2·10 ⁻¹¹	8.1·10 ⁻²²	4.7·10 ⁻²²	4.7·10 ⁻²²
2.78·10 ⁻²	1.3·10 ⁻¹⁰	1.3·10 ⁻¹⁰	9.8·10 ⁻¹³	6.4·10 ⁻²¹	6.4·10 ⁻²¹
2.78·10 ⁻¹	1.3·10 ⁻⁹	8.7·10 ⁻¹⁰	1.8·10 ⁻¹¹	1.9·10 ⁻¹⁸	1.9·10 ⁻¹⁸
2.78	1.2·10 ⁻⁸	1.2·10 ⁻⁹	5.4·10 ⁻¹⁰	3.5·10 ⁻¹⁷	3.5·10 ⁻¹⁷

Table 5Initial hydrogen pressures required to suppress UO₂ oxidative dissolution as a function of ε-particle surface coverage and dose rate with ks7 = 10² M⁻¹ s⁻¹ and ks6 = 50 M⁻¹ s⁻¹.

D [Gy·s ⁻¹]	H ₂ pressure [bar]		
	ε = 0.1%	ε = 1%	ε = 3%
2.78·10 ⁻⁵	0.0	0.0	0.0
2.78·10 ⁻⁴	0.0	0.0	0.0
2.78·10 ⁻³	1.7·10 ⁻³	0.0	0.0
2.78·10 ⁻²	4.4·10 ⁻²	5.7·10 ⁻³	0.0
2.78·10 ⁻¹	4.4·10 ⁻¹	1.7·10 ⁻¹	8.0·10 ⁻²
2.78	2.7	1.5	9.9·10 ⁻¹

3.1.2. Comparison to literature data

The impact of H₂ on the concentration of H₂O₂ upon alpha radiolysis has been explored experimentally by [Pastina and LaVerne \(2001\)](#), and was also discussed by [Trummer and Jonsson \(2010\)](#). The results of the simulations presented in this work are in line with the work by Pastina and LaVerne. In the work by Pastina and LaVerne, experiments clearly showed that H₂ (800 μM) has an insignificant effect on the H₂O₂ concentration upon irradiating an aqueous solution initially containing 50 μM H₂O₂ with 5 MeV He²⁺.

Experimental data on the impact of the reaction between H₂ and the surface-bound hydroxyl radical are not fully consistent. In a study by [Nilsson and Jonsson \(2008a\)](#), the kinetics for H₂O₂ consumption on UO₂-powder was studied in solutions containing 0 and 40 bar initial H₂. It is evident from these results that the kinetics for H₂O₂ consumption is not significantly affected by 40 bar H₂. The initial H₂O₂ concentration in this work was 0.22 mM which is roughly 150 times lower than the H₂ concentration. At H₂O₂ concentrations around 0.2 mM, the impact of the reaction between H₂O₂ and the surface-bound hydroxyl radical is very small. Hence, the experimental observation does not rule out a possible reaction between H₂ and the surface-bound hydroxyl radical. [Carbol et al. \(2009a\)](#), studied the effect of H₂ on the uranium dissolution from U-233 doped UO₂ and found that H₂ has a strong inhibiting effect. This effect could potentially be attributed to the reaction between H₂ and the surface-bound hydroxyl radical. However, the observed effect is much stronger than would be expected from the simulations carried out in this work. In the work by [Bauhn et al.](#), D₂ was found to inhibit radiation

induced oxidative dissolution of (U,Pu)O₂ were the α-particles originate from Pu ([Bauhn et al., 2018a](#)). As this material was unirradiated, noble metal inclusions are not present and the most likely explanation to the observed effect is the reaction between D₂ and surface-bound hydroxyl radical. The observed product, HDO, is also the product that would be expected from this reaction. However, it could also be formed from other reactions. [Hansson et al. \(2021\)](#) studied α-radiation induced oxidative dissolution of UO₂ under Ar and 10 bar H₂, respectively. The α-source was external and was separated by 30 μm from the UO₂ pellet. H₂ was found to reduce the oxidative dissolution also in this case and the most probable reason for this is again the reaction between H₂ and the surface-bound hydroxyl radical. The rate of oxidative dissolution is reduced by one order of magnitude which is well in line with our simulated results.

In addition to the experimental studies mentioned above there are numerous studies where noble metal inclusions are present. [Broczkowski et al.](#) have studied SIMFUEL containing various concentrations of noble metal inclusions using electrochemical techniques ([Broczkowski et al., 2005, 2007](#)). These studies have clearly shown that the corrosion potential is greatly reduced by H₂ for pellets containing noble metal inclusions. The response at a given H₂ pressure is proportional to the number density of the noble metal inclusions. [Bauhn et al. \(2018b\)](#), studied a SIMFUEL pellet with 339 mm² surface area, ~2% ε-particles ([Lucuta et al., 1991](#)), in 100 mL 10 mM NaHCO₃ with an initial concentration of 2.5 mM H₂O₂ at a D₂ pressure of 10 bar over approximately 150 h. An oxidation yield (defined as the amount of dissolved uranium per amount of consumed H₂O₂) of 1.69·10⁻⁴ was obtained. This implies that the oxidative dissolution was effectively inhibited which is perfectly in line with the model used in the simulations. [Carbol et al.](#) studied the impact of H₂ on the leaching of irradiated MOX fuel as well high burn-up structured UO₂ fuel ([Fors et al., 2009; Carbol et al., 2009b](#)). In both cases, dissolution was completely inhibited by H₂. In these cases, the inhibition can most probably be attributed to the noble metal inclusions. More recently, [Ekeröth et al.](#) demonstrated that H₂ can inhibit radiation induced dissolution of UO₂-based fuel already at low pressures ([Ekeröth et al., 2020](#)). The fact that radiolytic H₂ production is sufficient to stop the uranium dissolution has been confirmed in spent nuclear fuel leaching experiments where gases are not allowed to escape the reaction vessel, i.e., in sealed ampoules ([Eriksen and Jonsson, 2007](#)).

4. Conclusions

In this work we have incorporated two different surface processes accounting for H₂ inhibition of radiation induced dissolution of UO₂-based fuel in a numerical model recently developed. The two processes are the reaction between H₂ and the surface-bound hydroxyl radical which prevents oxidation of UO₂ and noble metal particle catalyzed H₂-reduction of U(VI) on the UO₂ surface. The rate constants for the two processes were assessed based on existing literature data. Based on simulations we were able to assess the relative impact of the two processes and it turned out that the noble metal inclusion catalyzed process is by far the most efficient one. Simulations show that even radiolytically produced H₂ is sufficient to completely stop radiation induced oxidative dissolution of UO₂-based fuel, perfectly in line with experimental

finding. The successful inclusion of these two surface processes into the model opens up for more detailed studies of the impact of other groundwater constituents.

Author statement

N.L. Hansson: Conceptualization, Formal analysis, Investigation, Methodology, Software, Validation, Visualization, Writing – original draft. M. Jonsson: Conceptualization, Methodology, Project administration, Supervision, Validation, Writing – review & editing.

Declaration of competing interest

The authors declare the following financial interests/personal relationships which may be considered as potential competing interests: Mats Jonsson reports financial support was provided by Swedish Nuclear Fuel and Waste Management Co.

Data availability

Data will be made available on request.

Acknowledgements

The Swedish Nuclear Fuel and Waste Management Company (SKB) is gratefully acknowledged for financial support.

References

- Barreiro Fidalgo, A., Kumagai, Y., Jonsson, M., 2018. The role of surface-bound hydroxyl radicals in the reaction between H_2O_2 and UO_2 . *J. Coord. Chem.* 71, 1799–1807.
- Bauhn, L., Hansson, N., Ekberg, C., Fors, P., Delville, R., Spahiu, K., 2018a. The interaction of molecular hydrogen with α -radiolytic oxidants on a (U,Pu) O_2 surface. *J. Nucl. Mater.* 505, 54–61.
- Bauhn, L., Hansson, N., Ekberg, C., Fors, P., Spahiu, K., 2018b. The fate of hydroxyl radicals produced during H_2O_2 decomposition on a SIMFUEL surface in the presence of dissolved hydrogen. *J. Nucl. Mater.* 507, 38–43.
- Bonin, B., Colin, M., Dufloy, A., 2000. Pressure building during the early stages of gas production in a radioactive waste repository. *J. Nucl. Mater.* 281, 1–14.
- Broczkowski, M., Noël, J., Shoesmith, D., 2005. The inhibiting effects of hydrogen on the corrosion of uranium dioxide under nuclear waste disposal conditions. *J. Nucl. Mater.* 346, 16–23.
- Broczkowski, M., Noël, J., Shoesmith, D., 2007. The influence of dissolved hydrogen on the surface composition of doped uranium dioxide under aqueous corrosion conditions. *J. Electroanal. Chem.* 602, 8–16.
- Carbol, P., Cobos-Sabate, J., Glatz, J., Ronchi, C., Rondinella, V., Wegen, D., Wiss, T., Loida, A., Metz, V., Kienzler, B., 2005. The Effect of Dissolved Hydrogen on the Dissolution of ^{233}U -Doped UO_2 (S), High Burn-Up Spent Fuel and MOX Fuel. Swedish Nuclear Fuel and Waste Management Company. Technical Report TR-05-09.
- Carbol, P., Fors, P., Gouder, T., Spahiu, K., 2009a. Hydrogen suppresses UO_2 corrosion. *Geochim. Cosmochim. Acta* 73, 4366–4375.
- Carbol, P., Fors, P., Van Winckel, S., Spahiu, K., 2009b. Corrosion of irradiated MOX fuel in presence of dissolved H_2 . *J. Nucl. Mater.* 392, 45–54.
- Christensen, H., Sehested, K., Corfitzen, H., 1982. Reactions of hydroxyl radicals with hydrogen peroxide at ambient and elevated temperatures. *J. Phys. Chem.* 86, 1588–1590.
- Christensen, H., Sehested, K., 1983. Reaction of hydroxyl radicals with hydrogen at elevated temperatures. Determination of activation energy. *J. Phys. Chem.* 87, 118–120.
- Cui, D., Ekeröth, E., Fors, P., Spahiu, K., 2008. Surface mediated processes in the interaction of spent fuel or alpha-doped UO_2 with H_2 . *Mater. Res. Soc. Symp. Proc.* 87–99.
- Ekeröth, E., Roth, O., Jonsson, M., 2006. The relative impact of radiolysis products in radiation induced oxidative dissolution of UO_2 . *J. Nucl. Mater.* 355, 38–46.
- Ekeröth, E., Granfors, M., Schild, D., Spahiu, K., 2020. The effect of temperature and fuel surface area on spent nuclear fuel dissolution kinetics under H_2 atmosphere. *J. Nucl. Mater.* 531, 151981.
- Eriksen, T.E., Jonsson, M., Merino, J., 2008. Modelling of time resolved and long contact time dissolution studies of spent nuclear fuel in 10 mM carbonate solution—a comparison between two different models and experimental data. *J. Nucl. Mater.* 375, 331–339.
- Eriksen, T., Jonsson, M., 2007. The Effect of Hydrogen on Dissolution of Spent Fuel in 0.01 Mol/dm³ NaHCO_3 Solution. Swedish Nuclear Fuel and Waste Management Co.
- Fors, P., Carbol, P., Van Winckel, S., Spahiu, K., 2009. Corrosion of high burn-up structured UO_2 fuel in presence of dissolved H_2 . *J. Nucl. Mater.* 394, 1–8.
- Hansson, N., Tam, P., Ekberg, C., Spahiu, K., 2021. XPS study of external α -radiolytic oxidation of UO_2 in the presence of argon or hydrogen. *J. Nucl. Mater.* 543, 152604.
- Hansson, N., Jonsson, M., Ekberg, C., Spahiu, K., 2023. Modelling radiation-induced oxidative dissolution of UO_2 -based spent nuclear fuel on the basis of the hydroxyl radical mediated surface mechanism: exploring the impact of surface reaction mechanism and spatial and temporal resolution. *J. Nucl. Mater.* 578, 154369.
- Hossain, M.M., Ekeröth, E., Jonsson, M., 2006. Effects of HCO_3^- on the kinetics of UO_2 oxidation by H_2O_2 . *J. Nucl. Mater.* 358, 202–208.
- Jonsson, M., 2010. Radiation-induced processes at solid-liquid interfaces. *Recent Trend. Radiat. Chem.* 301–323.
- Lawless, D., Serpone, N., Meisel, D., 1991. Role of hydroxyl radicals and trapped holes in photocatalysis. A pulse radiolysis study. *J. Phys. Chem.* 95, 5166–5170.
- Li, J., Liu, X., Jonsson, M., 2023. Exploring the change in redox reactivity of UO_2 induced by exposure to oxidants in HCO_3^- solution. *Inorg. Chem.* 62, 7413–7423.
- Lucuta, P., Verrall, R., Matzke, H., Palmer, B., 1991. Microstructural features of SIMFUEL—simulated high-burnup UO_2 -based nuclear fuel. *J. Nucl. Mater.* 178, 48–60.
- Maier, A.C., Jonsson, M., 2019. Pd-Catalyzed surface reactions of importance in radiation induced dissolution of spent nuclear fuel involving H_2 . *ChemCatChem* 11, 5108–5115.
- Muzeau, B., Jégou, C., Delaunay, F., Broudic, V., Brevet, A., Catalette, H., Simoni, E., Corbel, C., 2009. Radiolytic oxidation of UO_2 pellets doped with alpha-emitters (^{238}Pu). *J. Alloys Compd.* 467, 578–589.
- Nilsson, S., Jonsson, M., 2008a. On the catalytic effects of UO_2 (s) and Pd (s) on the reaction between H_2O_2 and H_2 in aqueous solution. *J. Nucl. Mater.* 372, 160–163.
- Nilsson, S., Jonsson, M., 2008b. On the catalytic effect of Pd (s) on the reduction of UO_2^{2+} with H_2 in aqueous solution. *J. Nucl. Mater.* 374, 290–292.
- Olsson, D., Li, J., Jonsson, M., 2022. Kinetic effects of H_2O_2 speciation on the overall peroxide consumption at UO_2 -water interfaces. *ACS Omega* 7, 15929–15935.
- Pastina, B., LaVerne, J.A., 2001. Effect of molecular hydrogen on hydrogen peroxide in water radiolysis. *J. Phys. Chem. A* 105, 9316–9322.
- Röllin, S., Spahiu, K., Eklund, U.-B., 2001. Determination of dissolution rates of spent fuel in carbonate solutions under different redox conditions with a flow-through experiment. *J. Nucl. Mater.* 297, 231–243.
- Trummer, M., Nilsson, S., Jonsson, M., 2008. On the effects of fission product noble metal inclusions on the kinetics of radiation induced dissolution of spent nuclear fuel. *J. Nucl. Mater.* 378, 55–59.
- Trummer, M., Roth, O., Jonsson, M., 2009. H_2 inhibition of radiation induced dissolution of spent nuclear fuel. *J. Nucl. Mater.* 383, 226–230.
- Trummer, M., Jonsson, M., 2010. Resolving the H_2 effect on radiation induced dissolution of UO_2 -based spent nuclear fuel. *J. Nucl. Mater.* 396, 163–169.
- Zanonato, P.L., Di Bernardo, P., Szabó, Z., Grenthe, I., 2012. Chemical equilibria in the uranyl (VI)-peroxide-carbonate system; identification of precursors for the formation of poly-peroxometallates. *Dalton Trans.* 41, 11635–11641.